

The role of excited species in ultraviolet-laser materials ablation III. Non-stationary ablation of organic polymers

B. Luk'yanchuk*, N. Bityurin**, S. Anisimov***, N. Arnold, D. Bäuerle

Angewandte Physik, Johannes-Kepler-Universität Linz, A-4040 Linz, Austria
(Fax: + 43-732/24689242)

Received: 3 January 1996/Accepted: 8 January 1996

Abstract. The role of non-stationary effects in nano-second ultraviolet (UV) excimer-laser ablation of organic polymers is discussed. The model includes reversible changes in absorption related to darkening and bleaching effects. Comparison of calculations and experimental data for polyimide demonstrates that the photophysical model describes the ablation kinetics quite well.

PACS: 82.65; 82.50; 42.10

The physical mechanisms involved in ultraviolet (UV)-laser polymer ablation are still under discussion [1–6]. With the bond energies of organic polymers which are, typically, around 3–5 eV [7] an explanation of the observed ablation rates on the basis of a purely thermal model would require very high surface temperatures, about $(6–10) \times 10^3$ K for fluences near the ablation threshold, Φ_{th} [8, 9]. Such high temperatures are in contradiction to experimental data on the vibrational temperature of ablation products [1] and to direct temperature measurements [3]. The latter reveal, for polyimide (PI) and 248 nm KrF-laser radiation ($\tau_l = 20$ ns FWHM) at fluences $\Phi \approx 36 \text{ mJ/cm}^2 \leq \Phi_{th}$, approximately 1660 K. On the other hand, the ablated thickness per pulse, Δh , derived from mass loss measurements on PI [4] near and below the ablation threshold, shows an Arrhenius-type behavior

$$\Delta h = A \exp \left[-\frac{B}{\Phi} \right], \quad (1)$$

*On leave from: General Physics Institute, Russian Academy of Sciences, 117942 Moscow, Russia

**On leave from: Institute of Applied Physics, Russian Academy of Sciences, 603600 Nizhni Novgorod, Russia

***On leave from: L.D. Landau Institute for Theoretical Physics, Russian Academy of Sciences, 117940 Moscow, Russia

where A and B depend on wavelength only. Equation (1) provides a good approximation for KrF-, XeCl- and XeF-laser radiation [4]. However, the activation energies derived, $\Delta E \propto B$, appear to be unreasonably small. For example, with the data for 248 nm laser radiation, one obtains $\Delta E \approx 0.7$ eV. With this value, the sublimation rate at $T = 300^\circ\text{C}$ would be about 10 cm/s. This is in obvious contradiction to the good thermal stability of PI. For 193 nm ArF-laser radiation the “photochemical law”

$$\Delta h = \alpha^{-1} \ln \left[\frac{\Phi}{\Phi_{th}} \right] \quad \text{with } \Phi \geq \Phi_{th}, \quad (2)$$

(α is the absorption coefficient) seems to be more appropriate [4]. Thus, the experiments indicate that the “red boundary” for mainly photochemical ablation of PI is somewhere between 193 and 248 nm. This would be in agreement with the assumption that photochemical ablation is related to the breaking of two C–N bonds. The corresponding energy (broken line) together with singlet energy levels in PI [10, 11] and the photon energies of various lasers is shown in Fig. 1. From the preceding considerations it becomes evident that an explanation of the experimental data in [3, 4] on the basis of either purely photochemical or purely thermal mechanisms is impossible.

Recent investigations have shown, however, that the experimental data on PI presented in [3, 4] can be described in terms of a *photophysical* ablation model [5, 6] which assumes a decrease in activation energy for the ablation (evaporation) of electronically excited species [12]. The present paper extends these studies to non-stationary regimes. Here, we consider instead of a two-level system [13] a four-level system which permits consideration of both bleaching [14–16] and darkening [17–19] effects. Temperature dependences of the specific heat, thermal conductivity, and of the absorption coefficient are ignored. The calculations were carried out for different laser wavelengths. They permit a direct comparison of theoretical results with experimental data [3, 4]. It should be noted that the influence of volatile species generated within the bulk of the material has *not* been taken into

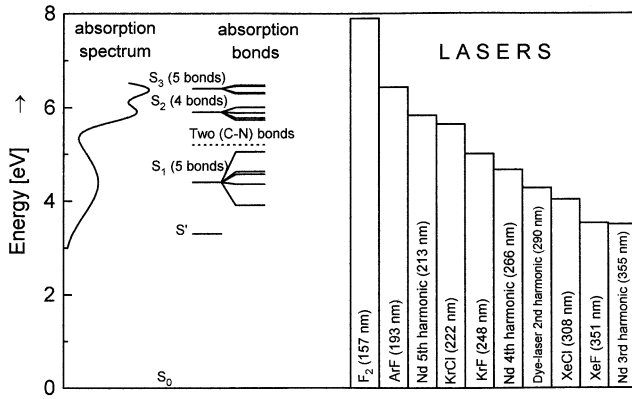


Fig. 1. Optical absorption spectrum and calculated [10, 11] positions of singlet energy levels for polyimide (DuPont Kapton). The absorption peaks are located at 4.4 eV (S_1), 5.9 eV (S_2) and 6.4 eV (S_3). The weak absorption peak (S') (not shown) at 3.3 eV is associated with an intramolecular charge-transfer transition. The bond breaking energy for two C–N bonds is also included

account. Gas losses which may not cause any changes in surface profile may, however, explain the Arrhenius tail observed in the mass loss measurements [4]. An analysis of data along these lines will be presented elsewhere.

1 Model

The model employed in the present calculations is shown in Fig. 2. Here, in analogy to [18, 19], we consider successive excitations $N_0 \rightarrow N_1$ and $N^* \rightarrow N_2$ with cross-sections σ_{01} and σ_{12} , respectively. The excitation–relaxation channels are:

- Excitation of level N_1 by absorption of photons with energy $h\nu$.
- Fast relaxation ($\tau_1 \rightarrow 0$) from N_1 to N^* , where N^* is either a singlet or a triplet level with longer relaxation time. Incorporation of this level permits the exclusion stimulated emission, which seems to be insignificant in the UV-laser interaction with PI.
- Absorption of a second photon $h\nu$ via the transition $N^* \rightarrow N_2$ and the relaxation $N_2 \rightarrow N^*$ where τ_2 shall be small compared to the thermal relaxation time, t_T .

With these conditions, the additional two levels, N^* and N_2 , lead only to changes in the absorption behavior and, hence, in the heat source term. The change in absorption is characterized by the additional parameter $s = \sigma_{12}/\sigma_{01}$. If we ignore the motion of the ablation front, the stationary solution of the kinetic equations for the population of the energy levels in Fig. 2 yields:

$$\alpha = \alpha_0 \frac{1 + sq}{1 + q}, \quad \text{where } q = \frac{I\sigma_{01}t_T}{h\nu}, \quad (3)$$

where α_0 is the linear absorption coefficient for low intensities ($q \rightarrow 0$). With $s > 1$, the absorption coefficient increases with intensity (darkening), while with $s < 1$, α decreases with intensity (bleaching). The four-level system permits to consider different types of electronic transitions at different wavelengths without significant refinements.

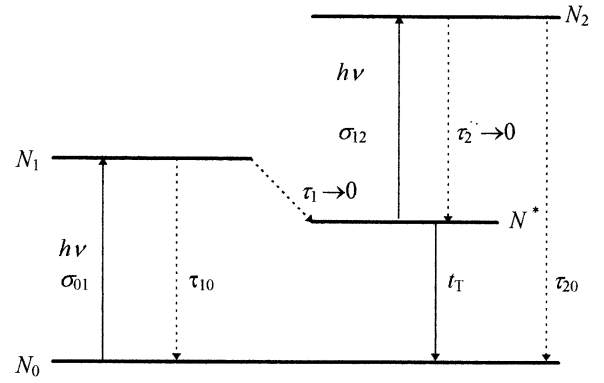


Fig. 2. Electronic transitions and relaxation channels considered in the calculations. Fast ($\tau_1, \tau_2 \ll t_T, \tau_{ex}$) and slow ($\tau_{10}, \tau_{20} \gg t_T, \tau_{ex}$) relaxation processes are indicated. $\tau_{ex} \sim h\nu/I\sigma$ is the excitation time

The equations for the concentration of excited species N^* , laser intensity I , and temperature T , can be written analogous to [5, 13] as

$$\frac{\partial N^*}{\partial t} = v \frac{\partial N^*}{\partial z} + (N - N^*) \frac{I\sigma_{01}}{h\nu} - \frac{N^*}{t_T}, \quad (4)$$

$$\frac{\partial I}{\partial z} = -I\sigma_{01}[N + (s - 1)N^*], \quad (5)$$

$$\frac{\partial T}{\partial t} = v \frac{\partial T}{\partial z} + D_T \frac{\partial^2 T}{\partial z^2} + \left(I\sigma_{01}s + \frac{h\nu}{t_T} \right) \frac{N^*}{\rho c_p}. \quad (6)$$

The ablation velocity $v = v(t)$ is given by

$$v = \left(1 - \frac{N_s^*}{N} \right) v_A \exp \left[-\frac{\Delta E}{T_s} \right] + \frac{N_s^*}{N} v_A^* \exp \left[-\frac{\Delta E^*}{T_s} \right], \quad (7)$$

where ΔE and ΔE^* are activation energies for the ground state, N_0 , and the excited state, N^* , respectively. N is the total number density of absorbing species (chromophores). The subscript s refers to the ablation front at $z = 0$. The boundary conditions can be written in the form

$$\kappa \frac{\partial T}{\partial z} \Big|_{z=0} = \left[\left(1 - \frac{N_s^*}{N} \right) v_A \Delta H \exp \left[-\frac{\Delta E}{T_s} \right] + \frac{N_s^*}{N} v_A^* \Delta H^* \exp \left[-\frac{\Delta E^*}{T_s} \right] \right] \rho \quad (8)$$

$$I|_{z=0} = I_0(t) \exp \left[-\alpha_g \int_0^t v(t_1) dt_1 \right]; \quad N^*|_{z \rightarrow \infty} = 0;$$

$$T|_{z \rightarrow \infty} = T_\infty. \quad (9)$$

Here, $\kappa = D_T c_p \rho$ is the thermal conductivity, while ΔH and ΔH^* are the corresponding enthalpies. The initial conditions are

$$N^*|_{t=0} = 0, \quad T|_{t=0} = T_\infty. \quad (10)$$

The intensity in (9) takes into account the shielding of the incident laser radiation by ablation products. Here, α_g is the absorption coefficient within the plume recalculated to the depth of the ablated material. $I_0(t)$ is the time-dependent laser-light intensity.

2 Numerical calculations and results

Steady-state solutions of (4)–(10) for a two-level system and $I = \text{const.}$ were studied in [5]. They are in *qualitative* agreement with experiments. The time, τ_s , required to reach the steady state can be estimated from [20]

$$\tau_s = \max\{D_T/v_s^2, 1/\alpha_0 v_s\},$$

where v_s is the steady-state velocity of the ablation front. In typical experiments with UV excimer lasers, the pulse duration, τ_l , is comparable or shorter than τ_s . Thus, a *quantitative* description of laser ablation cannot be performed on the basis of steady-state solutions.

For a comparison with experimental data, (4)–(10) were solved numerically by using the finite element method [21]. The parameters employed are listed in Table 1. D_T , c_p , ρ , and α_0 were taken from the literature. Values of N , ΔE , v_A , and ΔH were estimated on the basis of the experimental data presented in [7, 14]. Changes in ΔE , v_A , and ΔH within physically reasonable ranges did not significantly influence the results. v_A^* , ΔH^* , ΔE^* , t_T , α_g , and s were used as fitting parameters to experimental curves. These parameters were varied only within physically admissible ranges, except those for the 193 nm data. The activation energy derived, ΔE^* , is in good agreement with representative values for organic molecules [12]. The values $v_A \approx v_A^* \approx 10^6$ cm/s correspond approximately to molecular vibrational frequencies of about 10^{13} s $^{-1}$ and monomer sizes of about 10 Å.

Bleaching (darkening) strongly influences the laser ablation kinetics. This can be seen from the asymptotic ($t \rightarrow \infty$) profiles of the intensity obtained for different values of parameters s . When the motion of the ablation front is ignored, the stationary profiles obtained from (4) and (5) are given by

$$\ln \left\{ \frac{I}{I_0} \left[\frac{1 + st_T I \sigma_{01} / h\nu}{1 + st_T I_0 \sigma_{01} / h\nu} \right]^{(1-s)/s} \right\} = -z\alpha_0. \quad (11)$$

Such profiles are shown in Fig. 3. The time required to establish stationary conditions increases with decreasing s . Thus, even when heat conduction is ignored, the time of transient ablation depends on λ via s .

The ablated thickness per pulse depends on both the total fluence and the temporal shape of the laser pulse. For example, for PI the ablated layer thickness calculated for rectangular pulses exceeds that for triangular pulses of the same total energy and duration by more than 10%. Figure 4 shows T_s , v , and N_s^* for a triangular laser pulse. The thermal relaxation time was assumed to be 800 ps. The temporal dependence of $N_s^*(t)$ is close to the laser pulse shape with FWHM $\tau_l = 15$ ns. The maxima in the surface temperature and the ablation velocity are reached *after* the maximum in the laser intensity. The characteristic time for the decrease in surface temperature $T_s(t)$ is significantly longer than τ_l .

The ablation rates calculated from (4)–(10) for the same triangular laser pulse and for different laser wavelengths are shown in Fig. 5a, b by the *full* curves. The experimental data have been taken from [4]. The accu-

Table 1. Parameters employed in numerical calculations

	$\lambda = 193$ nm	$\lambda = 248$ nm	$\lambda = 308$ nm	$\lambda = 351$ nm
ΔE , eV	3	3	3	3
ΔE^* , eV	1.9	1.27	1.47	1.54
v_A , cm/s	10^6	10^6	10^6	10^6
v_A^* , cm/s	6.5×10^7	5.7×10^5	8.3×10^5	5.36×10^6
ΔH , J/g	2.3×10^3	2.3×10^3	2.3×10^3	2.3×10^3
ΔH^* , J/g	0	7.4×10^2	8.5×10^2	4.3×10^2
$\alpha_0 = \sigma_{01} N$, cm $^{-1}$	3.4×10^5	3×10^5	8.6×10^4	3.6×10^4
α_g , cm $^{-1}$	1.7×10^5	1.56×10^5	4.3×10^4	0
t_T , ps	18200	528	800	179
s	20	0	17	21.7
c_p , J/g K	1.1	1.1	1.1	1.1
ρ , g/cm 3	1.42	1.42	1.42	1.42
D_T , cm 2 /s	0.001	0.001	0.001	0.001
N , cm $^{-3}$	6×10^{21}	6×10^{21}	6×10^{21}	6×10^{21}
T_∞ , K	300	300	300	300

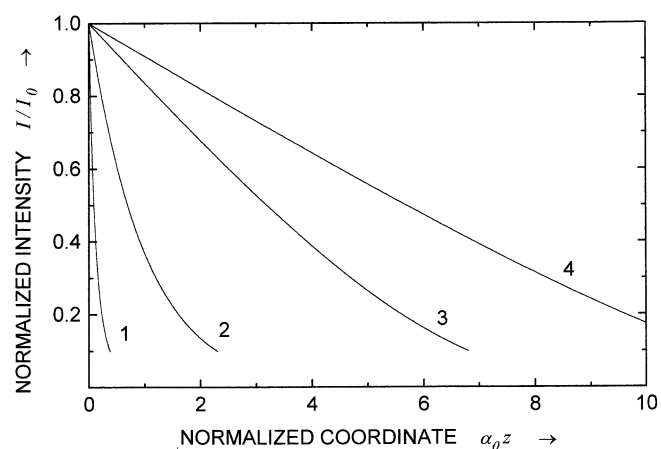


Fig. 3. Spatial profiles of normalized laser-light intensity for different values of the parameters s , I_0 and t_T : (1) $s = 10$, $I_0/I_b = 5$, $t_T/t_0 = 1$, (2) $s = 0$, $I_0/I_b = 5$, $t_T/t_0 = 0$, (3) $s = 0$, $I_0/I_b = 5$, $t_T/t_0 = 1$, (4) $s = 0$, $I_0/I_b = 10$, $t_T/t_0 = 1$. (Curve 2) shows Beer's law: $I = I_0 \exp(-\alpha_0 z)$, $I_b = 10^7$ W/cm 2 , $t_0 = h\nu/\sigma_{01} I_b$

racy of the fit becomes most evident in Fig. 5a and b for high and low fluences, respectively.

The activation energy derived, ΔE^* , depends on the details of the solution of the heat equation. If we assume the specific heat c_p and thermal diffusivity D_T to be constants, the fit to experimental data [4] yields ΔE^* ($\lambda = 248$ nm) = 1.27 eV. With low fluences, when bleaching effects and heat losses due to evaporation can be ignored, the maximum surface temperature is $T_{s \text{ max}} \propto \Phi$, and (1) is obtained. At higher fluences, bleaching (for $\lambda = 248$ nm) and heat losses result in a sublinear dependence of $T_{s \text{ max}}$ on fluence, and thereby in a decrease in slope in Fig. 5b. However, with $\alpha_g = 0$ the calculated change in slope is smaller than the experimentally observed one [4]. This discrepancy might be caused by the shielding of the incident laser radiation by ablation products ($\alpha_g \neq 0$).

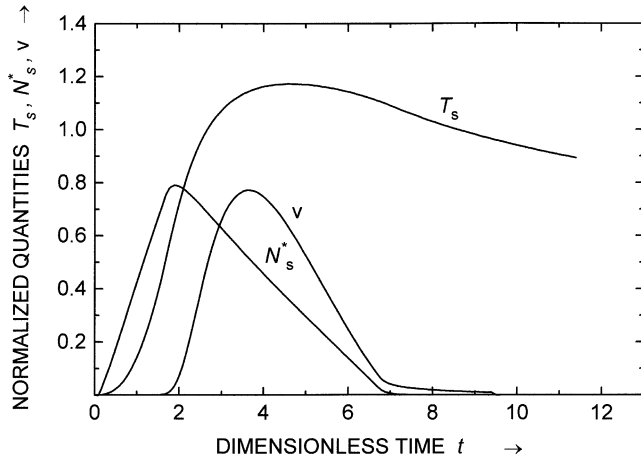


Fig. 4. Temporal dependences of normalised surface temperature T_s , surface concentration of excited species N_s^* , and ablation front velocity v for triangular XeCl-laser pulse, $\Phi = 75 \text{ mJ/cm}^2$ ($\lambda = 308 \text{ nm}$, $\tau_l = 15 \text{ ns}$ FWHM). A single dimensionless unit corresponds to $T_s = 2474 \text{ K}$, $N_s^* = 6 \times 10^{21} \text{ cm}^{-3}$, $v = 2.58 \times 10^3 \text{ cm/s}$, and $t = 4.47 \text{ ns}$

3 Interpolation formula

It is of interest to heuristically construct a simple interpolation formula. Let us assume that the maximum surface temperature $T_{s \text{ max}}$ is proportional to $\Phi \exp(-\alpha_f \Delta h)$ where $\alpha_f \neq \alpha_g$ is a fitting parameter. We then obtain [13]

$$\Phi = B \exp[\alpha_f \Delta h] \ln^{-1} \left[\frac{A}{\Delta h} \right]. \quad (12)$$

With fluences $\Phi \ll \Phi_{\text{th}}$, (12) can be transformed into the kinetic law (1). With fluences $\Phi \gg \Phi_{\text{th}}$, we obtain the logarithmic law (2) with $\Phi_{\text{th}} = B/\ln(\alpha_f A)$.

The dashed curves in Figs. 5a, b are the least-squares fit of experimental data by (12). Each specific curve is characterized by three parameters, A , B , and α_f . The values of these parameters, determined from the fit are listed in Table 2. It is interesting to note that the interpolation formula describes even the data for $\lambda = 193 \text{ nm}$, although the big difference in the coefficient A indicates a drastic change in the ablation process.

Another interesting effect can be seen for $\lambda = 351 \text{ nm}$. The parameter α_f in (12) is the only one which takes into account changes in absorption during ablation. α_f describes the *average* change in absorption, including bleaching and darkening. The negative value of α_f obtained with 351 nm XeF-laser radiation may be related to the plasma radiation which increases the overall energy absorbed within the polymer.

4 Discussion

The present calculations show that the maximal temperatures reached in UV-laser photophysical ablation are significantly lower than those derived from a purely ther-

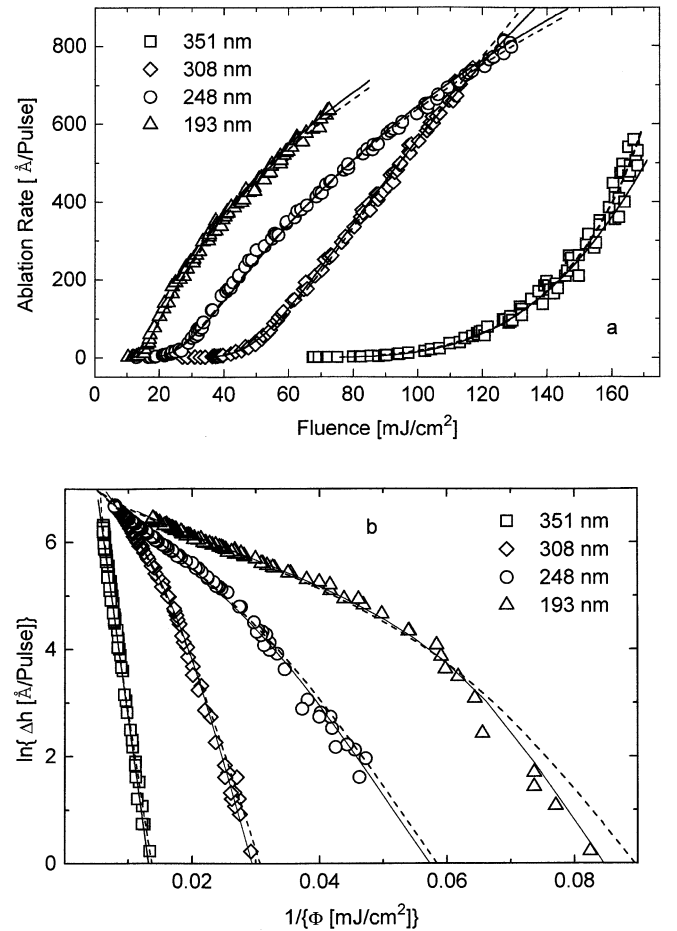


Fig. 5. (a) Ablated thickness Δh [$\text{\AA}/\text{Pulse}$] versus laser fluence Φ [mJ/cm^2] for laser ablation with different wavelengths. The experimental data are taken from [4]. Full curves were calculated by the solution of non-stationary problem (4)–(10) with parameters listed in Table 1. Dashed curves have been obtained from the interpolation formula (12). (b) Arrhenius plot of ablation rate

Table 2. Fitting parameters employed in interpolation formula (12)

λ [nm]	A [$\text{\AA}/\text{Pulse}$]	B [mJ/cm^2]	α_f [cm^{-1}]
193 (ArF)	883547	152.56	2×10^5
248 (KrF)	29716	176.13	1.22×10^5
308 (XeCl)	87097	370.03	5.5×10^4
351 (XeF)	32562	760.92	-1.9×10^4

mal model. This is caused by the small activation energies of electronically excited species, ΔE^* . For 248 nm our calculations yield $T_{s \text{ max}} < 2000 \text{ K}$ near the ablation threshold, in agreement with experimental data [3]. For 301 and 351 nm radiation, the temperature rise is somewhat higher. For XeCl-laser radiation and $\Phi = 75 \text{ mJ/cm}^2$, Fig. 4 yields $T_{s \text{ max}} \approx 2900 \text{ K}$. The ablation rate for this fluence is about $300 \text{ \AA}/\text{pulse}$ (Fig. 5). $T_{s \text{ max}}$, and thereby ΔE^* , decrease further if we take into account the temperature dependence in the specific heat and the heat diffusivity.

A numerical study of our model permits to explain the dependence of the ablation rate on fluence, as obtained in

[4] for $\lambda = 248, 308, 351$ nm. However, a fit of the data for $\lambda = 193$ nm leads to unreal values of parameters v_A^* , t_T , ΔH^* (Table 1). This indicates a significant change in ablation mechanisms.

The values of relaxation times t_T derived from the fit are listed in Table 1. The only experimental data available [18] give $t_T \sim 34$ ps for $\lambda = 355$ nm which is much shorter than that suggested by our model. This question should be clarified further in detail.

The dependence of Φ_{th} on laser pulse duration has been studied as well. With 10^{-8} s $< \tau_l < 10^{-5}$ s this dependence can be approximately by $\Phi_{th} \propto \tau_l^\beta$, where $\beta = 0$ stands for a purely photochemical process, and $\beta = 0.5$ for a purely thermal process. Our calculations show that for photophysical ablation $\beta \approx 0.5$ (the exact value depends on s and on the temperature dependence of parameters).

5 Conclusion

Experimental data on excimer-laser ablation of PI can semiquantitatively be explained on the basis of non-stationary photophysical ablation by taking into account changes in absorption due to bleaching or darkening. The model permits to explain the following experimental results:

- Arrhenius-like behavior for subthreshold fluences $\Phi < \Phi_{th}$.
- Activation energies that are considerably smaller than bond breaking energies.
- Fairly high ablation rates at relatively low surface temperatures.
- The absence of certain types of surface instabilities [6].

The experimental results can be described as well by a semiempirical formula which takes into account the shielding of the incident radiation by ablation products.

Acknowledgements. The authors are grateful to Dr. J. Brannon for the presentation of the numerical file with experimental data [4] and

to the Russian Basic Research Foundation and the “Fonds zur Förderung der wissenschaftlichen Forschung in Österreich” for financial support. Part of this work was also supported by INTAS (grant 94-902) and ISF (grant JAW 100, R89000, R89300).

References

1. R. Srinivasan: In *Laser Ablation. Principles and Applications*, ed. by J.C. Miller, Springer Ser. Mater. Sci. Vol. 28 (Springer, Berlin, Heidelberg 1994) p. 107
2. S. Lazare, V. Granier: *Laser Chem.* **10**, 25 (1989)
3. D.P. Brunco, M.Q. Thompson, C.E. Otis, P.M. Goodwin: *J. Appl. Phys.* **72**, 434 (1992)
4. S. Küper, J. Brannon, K. Brannon: *Appl. Phys. A* **56**, 43 (1993)
5. B. Luk'yanchuk, N. Bityurin, S. Anisimov, D. Bäuerle: *Appl. Phys. A* **57**, 367 (1993); *Int'l Conf. ALT'92*, Moscow (1992)
6. B. Luk'yanchuk, N. Bityurin, S. Anisimov, D. Bäuerle: *Appl. Phys. A* **57**, 449 (1993)
7. J. Guillet: *Polymers – Photophysics and Photochemistry. An Introduction to the Study of Photoprocesses in Macromolecules* (Cambridge Univ. Press, Cambridge 1985)
8. D. Bäuerle, B. Luk'yanchuk, P. Schwab, X.Z. Wang, E. Arenholz: In *Laser Ablation of Electronic Materials*, ed. by E. Fogarassy, S. Lazare (North-Holland, Amsterdam 1992) p. 39
9. S.R. Cain, F.C. Burns, C.E. Otis, B. Braren: *J. Appl. Phys.* **72**, 5172 (1993)
10. G. Arjavalingham, G. Hougham, J.P. LaFemina: *Polymer* **31**, 840 (1990)
11. J.P. LaFemina, G. Arjavalingham, G. Hougham: *J. Chem. Phys.* **90**, 5154 (1989)
12. V.G. Plotnikov: *Dokl. Akad. Nauk SSSR* **301**, 376 (1988)
13. B. Luk'yanchuk, N. Bityurin, S. Anisimov, D. Bäuerle: In *Excimer Lasers*, ed. by L.D. Laude, NATO ASI Series E **256**, 59 (Kluwer, Dordrecht, 1994)
14. R. Sauerbrey, G.H. Pettit: *Appl. Phys. Lett.* **55**, 421 (1989)
15. G.H. Pettit, R. Sauerbrey: *Appl. Phys. Lett.* **58**, 793 (1991)
16. G.H. Pettit, R. Sauerbrey: *Appl. Phys. A* **56**, 51 (1993)
17. J.H. Brannon, J.R. Lankard, A.I. Baise, F. Burns, J. Kaufman: *J. Appl. Phys.* **58**, 2036 (1985)
18. J.K. Frisoli, Y. Hefetz, T.F. Deutsch: *Appl. Phys. B* **52**, 168 (1991)
19. H. Fukumura, H. Masuhava: *Chem. Phys. Lett.* **221**, 373 (1994)
20. S.I. Anisimov: *High Temp.* **6**, 110 (1968)
21. O.C. Zienkiewicz: *The Finite Element Method* (McGraw-Hill, New York 1977)